PERGAMON

Planetary and Space Science 48 (2000) 617–636

Planetary and Space Science

www.elsevier.nl/locate/planspasci

On the internal structure and dynamics of Titan

O. Grasset*, C. Sotin, F. Deschamps

Laboratoire de Géophysique et Planétologie, 2, rue de la Houssinière, BP 92208, 44322, Nantes, Cedex 3, France

Received 10 December 1998; received in revised form 19 July 1999; accepted 20 August 1999

Abstract

The purpose of this paper is to study the evolution of Titan from the primordial core overturn to the present, and to investigate the possible existence of both a deep liquid layer and an iron core, depending on the composition of chondrites and the primordial amount of volatiles included in ices. Models of Titan's interior are constructed using theoretical models based on thermal and mechanical properties of ices and silicates. Depending on both the heat transfer efficiency in chondrites and ices, and the amount of heat present in the interior, many properties of the deep structure of the satellite are deduced. Heat transfer through the convecting shell in planets is commonly estimated using parameterized laws which relate the vigor of convection to the heat flux at the top of the convecting shell. These laws, established from studies with constant viscosity fluids have been changed in order to take into account the very large viscosity contrasts in the different layers. Models also require a good knowledge of both thermodynamic and rheological parameters of materials at high pressure. In Titan, many volatiles were probably present in the primordial liquid layer. These volatiles must decrease the freezing temperature of the liquid which is of fundamental importance for the evolution of the satellite. Recent experimental results on the system NH_3–H_2O are included in the present models.

Evolution of the core — Using numerical models incorporating recent results on thermal convection for fluids with strongly temperature dependent viscosity, the thermal evolution of Titan's core is presented for two possible compositions of the planetoids. In the first case, the chondritic part of the planetoids was possibly composed of CI chondrites and the core is simply composed of silicates, whereas in the second case, chondrites with a large amount of metallic iron (EH enstatite chondrites) were accreted during Titan's formation. Diffusive heating increases the averaged temperature of the homogeneous chondritic core up to a critical value where marginal convection may occur about 1 Ga after the core overturn. In case 1, the onset of convection is accompanied by partial melting of the silicate core. Then, the vigor of convection keeps increasing and would still be vigorous at the present time. Partial melting of silicates below a thick thermal boundary layer at the top is very likely at present. In the other model (case 2), metallic iron starts melting before the onset of convection and implies a rapid overturn of the chondritic core into a layered structure with a dense liquid iron core surrounded by a silicate layer. In this layered core, convection in the silicate layer is not very vigorous, but probably still exists.

Evolution of the icy layers — Radiogenic heating of silicates is transferred by convection through the ice shell. If convection is vigorous, the heat flux through the ice shell is larger than the heat flux from the core and crystallization in the liquid shell occurs both at the top and at the bottom. Then, two different evolutions can be expected: (i) the decrease of temperature due to thickening is small and the Rayleigh number of the ice I shell increases when the layer thickens (pure H_2O case). Freezing of the liquid layer is very rapid and Titan is presently composed of a thick icy mantle, which convects vigorously; and (ii) the freezing temperature decreases strongly when pressure increases so that the Rayleigh number does not increase when ice I thickens because viscosity increases rapidly (NH_3–H_2O case). As a consequence, the thickening of ice I is very slow. The present structure of Titan depends on the primordial composition of the liquid layer, but it is probable that a liquid layer, which could be more than 350 km thick, still exists in the interior of the satellite. Such a layer may be determined by the Cassini measurements. © 2000 Elsevier Science Ltd. All rights reserved.

* Corresponding author.

0032-0633/00/$ - see front matter
PII: S0032-0633(00)00039-8

1. Introduction

Titan, the largest satellite of Saturn, is one of the most striking objects of the solar system. With a mean density of roughly 1900 kg/m^3, Titan is composed of nearly equal mass fractions of silicates and ices. Its enormous size is comparable to Jupiter's moons Ganymede and Callisto, but it is the only icy satellite with a thick atmosphere. Voyager measurements showed the atmosphere to be mainly composed of nitrogen with a few percent of methane (Tyler et al., 1981; Hanel et al., 1981). Many organic species including hydrocarbons and nitriles must also be present (Sagan and Thompson, 1984; Thompson et al., 1991). Photochemical processes that occur in the atmosphere should lead to a rapid depletion in methane (Lunine, 1994) and it is possible that we are witnessing the last gasp of chemical processes in Titan's atmosphere. But the present abundance of methane could also indicate that a constant replenishment occurs at the surface of the satellite (Lunine, 1994). Such replenishment cannot be understood without an accurate knowledge of both Titan's surface and interior. Lunine (1993) gives an exhaustive review of our current understanding of Titan's surface. In this paper, recent experimental data on ices and numerical results on convecting fluids with variable viscosity will be used to provide a better understanding of the internal structure and dynamics of Titan.

Present data on Titan — atmospheric composition, mass, size, and density — are not sufficient to provide valuable information for describing accurately the internal structure. Seismic data or at least gravitational potential is required if one wants to constrain the interior of a planetary body. Valuable data about Titan's interior will be provided by flybys of Titan during the Cassini mission since accurate measurements of the quadrupole moments of Titan's gravity field will be made. Rappaport et al. (1997) have shown that these data will accurately constrain the internal structure of the satellite. The Cassini mission should allow us to determine if Titan is differentiated and if a deep liquid layer exists. In this paper, we propose to study Titan's interior using theoretical models based on thermal and mechanical properties of ices and silicates and on simple assumptions about the formation of the satellite. We will show that the models of Titan's structure depend mainly on the primordial composition of planetoids. Comparison of Cassini data with theoretical results will then provide valuable information about the formation of the saturnian system.

The first stages of Titan's history have been modeled in a previous study (Grasset and Sotin, 1996). Assuming that the accretion of Titan was homogeneous and very fast, its primordial structure was composed of three different layers: a core with a composition similar to planetoids (ices, hydrates, clathrates and chondrites); a layer of chondrites; and a liquid shell with a thin icy surface because of the cold subnebulae temperature (Lewis, 1971; Schubert et al., 1981; Cole, 1984; Lunine and Stevenson, 1987; Kuramoto and Matsui, 1994; Grasset and Sotin, 1996). Volumetric heating occurs in the primordial core through the decay of radiogenic elements included in chondrites. The temperature rises up to the melting temperature of ices. Once melting occurs in the core, tensional stresses increase at the bottom of the chondritic layer leading to its rupture and breaking up. Subsequent rock fragments migrate downwards. Finally, a core overturn is achieved after roughly 1.0 Ga leading to a pure chondritic core surrounded by a thick icy shell still rich in volatiles (Lunine and Stevenson, 1987). Kirk and Stevenson (1987) in the case of Ganymede first described this process of core overturn. Due to the similar sizes and densities of the two satellites, Lunine and Stevenson (1987) used the same model for Titan. Once accretion is achieved, Titan cools from above. Evolution of the primordial liquid layer can be deduced from the phase diagram of water ice (Fig. 1). Because of the cold temperature at the surface (93 $\pm$ 1 K), an outer ice I shell forms very rapidly above the liquid layer. The temperature profile in the liquid layer is adiabatic (dashed line in Fig. 1). High-pressure ices form at the bottom because the adiabatic profile crosses the melting curve of high-pressure polymorphs of ice. Initially,

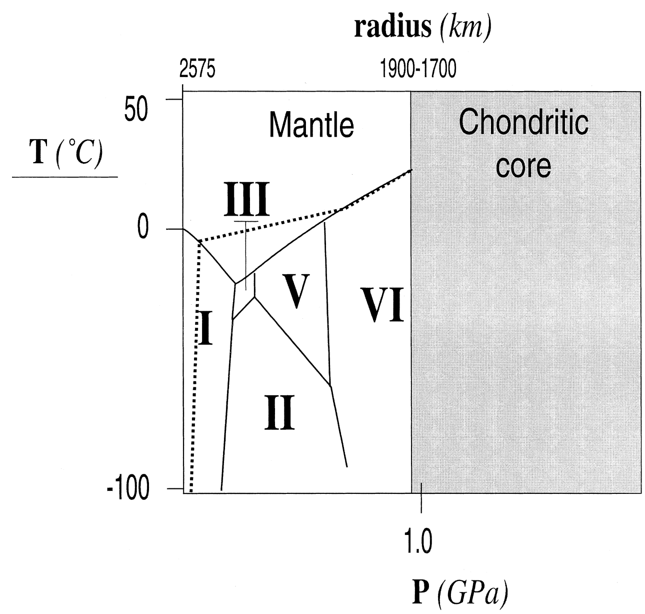

Fig. 1. The phase diagram of water ice. Above the chondritic core of Titan, many polymorphs of ice can be present due to the large range of pressure encountered. During the primordial freezing of the liquid layer, the thermal profile (dashed line) crosses the melting curves of both low- and high-pressure polymorphs.

the ice I layer is very thin (less than 1 km) and the conductive heat transfer is very important ($q = k_1 \Delta T/d \approx 400$ mW/m^2 with k_1, ΔT, and d, being thermal conductivity, temperature drop, and thickness of ice I, respectively), yielding a rapid cooling of the deep ocean. As the liquid cools down, the outer ice I shell thickens and conduction heat transfer decreases since it is inversely proportional to the thickness of the layer. Eventually, ice I thickens until its heat flux becomes equal to the heat flux from the core due to radiogenic heating. If this was the case, thickness would be roughly 50 km (Grasset and Sotin, 1996). Before it thickens so much, previous models (Reynolds and Cassen, 1979; Kirk and Stevenson, 1987; Grasset and Sotin, 1996) predict that the outer ice I layer becomes unstable to subsolidus convection, a mode of heat transfer much more efficient than conduction to cool down the interior of the satellite. If the liquid layer is pure water, convection in ice I is very vigorous (Lunine and Stevenson, 1987; Grasset and Sotin, 1996)

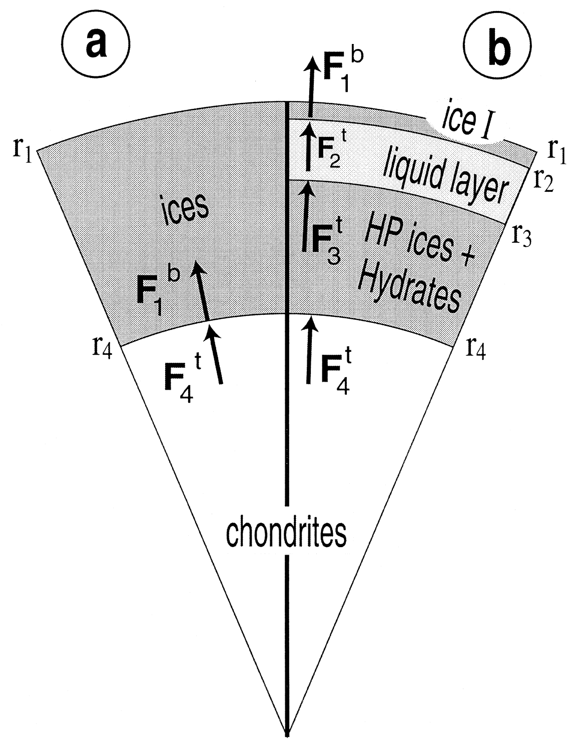

Fig. 2. Internal structure of Titan after the core overturn ($t_0 \sim 1$ Ga). (a) Pure water case: the liquid layer is frozen and a thick icy mantle surrounds the silicate core. (b) Volatile rich case: cooling of the liquid layer is slow because melting temperature is very low and heat transfer through ice I is small. A three-layered mantle is present after the core overturn. Symbols r and F are radii and heat flux, respectively. The subscripts are: (1) ice I layer or whole icy layer; (2) liquid layer; (3) high pressure icy layer; (4) chondritic core or silicate layer; and (5) iron inner core. Superscripts "t" and "b" are for top and bottom, respectively. For example, F_2^t is the heat flux at the top of the liquid layer.

and the liquid layer crystallizes before the end of the core overturn (Fig. 2(a)). On the other hand, if volatiles are incorporated in the liquid layer, a rapid cooling is not possible (Lunine and Stevenson, 1987; Grasset and Sotin, 1996) and a three layered mantle is present after the core overturn (Fig. 2(b)). In this paper, we will assume that the internal structure of Titan has been as it is sketched in Fig. 2 roughly 1 Ga after accretion. Our purpose is to study the evolution of Titan from 1 Ga to the present, and to investigate the possible existence of both a deep liquid layer and an iron core into Titan, depending on the composition of chondrites and the primordial amount of volatiles included in ices.

The internal structure and dynamics of icy satellites is commonly modeled using scaling laws which compute how much heat can be transferred from the interior to the surface (Consolmagno and Lewis, 1978; Reynolds and Cassen, 1979; Cassen et al., 1982; Lupo, 1982). Following Schubert et al. (1979), heat transfer through convecting shell in planets is commonly estimated using scaling laws, which relate the vigor of convection to the heat flux at the top of the convecting shell. These laws come from the Rayleigh–Benard type of convection and have been established from both laboratory and numerical experiments. In the Rayleigh–Benard regime, the fluid has a constant viscosity, and the shell is heated from below and cooled from above. The shell is limited by two thermal boundary layers, through which heat is transferred by conduction. The thickness of these layers is determined assuming that the temperature difference across the thermal boundary layer is half the total temperature difference. To account for the strongly temperature-dependent viscosity, previous models define the upper conductive lid by a cut-off temperature, reducing the temperature difference across the thermal boundary layers and therefore the viscosity of the convective layer. This way of modeling the thermal evolution of planets follows the suggestions of Nataf (1991) which state that the convective sublayer is almost isoviscous and obeys the same scaling laws than those for isoviscous fluids. Recent studies have shown that the temperature variations across the thermal boundary layers depend on a viscous temperature scale (Davaille and Jaupart, 1993; Moresi and Solomatov, 1995; Solomatov, 1995; Grasset and Parmentier, 1998; Deschamps and Sotin, 2000). In this paper, we use these new results to investigate the thermal evolution of Titan.

Models also require a good knowledge of both thermodynamic and rheological parameters of materials at high pressure. In Titan, many volatiles were probably present in the primordial liquid layer (Lunine and Stevenson, 1987). These volatiles must decrease the freezing temperature of the liquid which is of fundamental importance for the evolution of the satellite (Consolmagno and Lewis, 1978; Lunine and Stevenson, 1987; Grasset and Sotin, 1996; Sotin et al., 1998). Recent experimental results on the system NH_3–H_2O (Hogenboom et al., 1997; Grasset et al., 1995) will be used for the present study. The dynamics of icy satellites also depend strongly on the rheology of ices (Poirier, 1982). Many studies have been carried out (Poirier et al., 1981; Friedson and Stevenson, 1983; Kirby et al., 1985; Sotin et al., 1985; Echelmeyer and Kamb, 1986; Sotin and Poirier, 1987; Kargel et al., 1991; Duhram et al., 1993; Goldsby and Kolhstedt, 1997) and provide a good estimate of the viscosity of ices at the low stresses which must exist in convecting icy mantles. These data, and especially the recently published data on the viscosity of ice I (Goldsby and Kolhstedt, 1997) are incorporated in the models presented in this study.

Thermal evolution of Titan after the core overturn (Fig. 2) up to the present will be described. This evolution depends on the amount of heat that escapes from the chondritic core and on the efficiency of heat transfer through the icy mantle. In the first part, possible structure and dynamics of the silicate core will be presented. Estimates of the heat flux expelled at the bottom of the deep icy layer will be provided. Evolution of the icy mantle will be studied in the second part and the role played by volatiles will be pointed out.

2. Evolution of the chondritic core

2.1. Composition of the core

Planetoids which accreted to form Titan can be split into a chondritic part (silicates + metallic iron) and an icy part. Since the core of Titan has been formed by the fall of dense materials after accretion, its composition may be estimated from the nature of the chondrites included in planetoids. The problem is that the primordial composition of planetoids before the accretion of Titan is not known. CI chondrites, mainly composed of hydrated minerals (serpentine, epsomite, magnetite, troilite, and gypsum) have an elemental abundance that fits well in solar abundance. Despite the fact that they probably did not originate from the nebula, they could be a good analog of the rocky part of icy satellites (Mueller and McKinnon, 1988). On the other hand, stable isotope and redox characteristics of the Earth are only well matched by EH enstatite chondrites (Javoy, 1995) which means that the composition of the planetoids at the origin of planets must not necessarily fit solar abundance. The enstatite chondrites have little or no oxidized iron and are composed almost exclusively of the high temperature mineral enstatite or clinoenstatite, free silica and/or oligoclase, iron and troilite. Two extreme cases will be studied. First, the chondritic part of the planetoids was possibly composed of CI chondrites and the core is simply composed of silicates assuming that the redox state of iron does not change with time due to the small pressure and temperature ranges reached during the internal evolution of the icy satellite. Second, chondrites with a large amount of metallic iron were possibly accreted during Titan's formation. In that case, the radius of the interface between the silicate shell and the icy mantle is smaller because metallic iron is much denser than iron bearing silicates. In addition, we will show that a present metallic iron core is plausible.

2.2. The CI chondrites case

2.2.1. Diffusive heating

If CI chondrites were a good analog of planetoids accreting on Titan, the core of Titan must be composed of pure silicates after the primordial overturn (Fig. 2) since CI chondrites are characterized by the lack of metallic iron. Taking estimates for physical parameters describing ices and silicates in Table 1, the mass of Titan provides a crude estimate of the radius of the core: $r_4 \approx 1870$ km.

Thermal evolution of the chondritic core is mainly controlled by the volumetric heating of radiogenic components incorporated in silicates and the cooling from the top due to the high-pressure ice shell (Fig. 2). Thermal diffusion in a volumetrically heated spherical shell cooled from above is a simple numerical problem (Carslaw and Jaeger, 1959). The shell is divided into a conductive thermal boundary layer at the top, which thickens roughly as $t^{1/2}$. Temperature in the interior T_i depends on both time and depth, but the depth dependence below the thermal boundary layer is negligible. The temperature difference that would exist if there were no thermal diffusion increases with time as:

$$T_i(t) - T_i(t_0) = \frac{H_0}{C_{p_4}} \frac{e^{-\lambda t_0} - e^{-\lambda t}}{\lambda}. \tag{1}$$

In Eq. (1), parameters are described in Table 1 except t_0, which is the time necessary for the overturn of the primordial core. H_0 is the integrated heat due to the decay of long-lived radiogenic elements at the formation of the solar system. H_0 and λ are fixed in order to fit the Earth mean mantle heat production rate due to the decay of radioactive isotopes (Turcotte and Schubert, 1982). The concentration of uranium and thorium are a factor of two larger than the chondritic values, but the concentration of potassium is a factor of three smaller. Then, the heat production rate is 25% smaller than the chondritic heating rate. This choice provides us with a very small heating rate in Titan's core. If either melting of iron or convection occurs in the core, this cannot be due to an overestimation of the heating rate. For $t_0 = 1$ Ga the core overturn is almost achieved (Lunine and Stevenson, 1987). The initial temperature $T(t_0)$ is difficult to estimate. Just after accretion, the averaged temperature in the primordial core composed of silicates and ices was probably not larger than 200 K (Grasset and Sotin, 1996). Before the core overturn, the volumetric heating by radiogenic decay was very intense, but the increase of temperature in silicates was probably not very large because an important part of this heat was used for melting the ice below the silicate cap (Kirk and Stevenson, 1987). Furthermore, silicates cooled during their fall towards the center since ices trapped in the primordial core were at temperatures as cold as 100 K (Grasset and Sotin, 1996). It is then reasonable to assume that the initial temperature was in the range 400–600 K. The exact value is not of fundamental importance because temperature increases by 100 K every 100 Ma at the beginning. Using parameters described in Table 1, Eq. (1) predicts an increase of temperature of 650 K from t_0 to $t_0 + 1$ Ga (Fig. 3). Two billion years after the core overturn, temperature may become larger than 1400 K in the deepest part of the core. At these temperatures, it is reasonable to

Table 1
Physical parameters describing Titan's layers

	Parameter	Unit	Value	Reference	Name
Titan	Radius	m	2.575×10^6	Morrison and Owen (1988)	r_1
	Gravity acceleration	m/s^2	1.35		g
	Surface temperature	K	93 ± 1	Samuelson et al. (1997)	T_s
Interfaces	Ice I–liquid	m	Variable		r_2
	Liquid–ice VI	m	Variable		r_3
	Ice VI–silicates	m	1.87×10^6	CI case	r_4
		m	1.71×10^6	EH case	r_4
	Silicates–iron	m	0.91×10^6	EH case	r_5
Ice I layer	Density	kg/m^3	917	Hobbs (1974)	ρ_1
	Heat conductivity	W/m/K	2.6	Hobbs (1974)	k_1
	Thermal diffusivity	m^2/s	1.47×10^{-6}	Hobbs (1974)	κ_1
	Expansion coefficient	K^{-1}	1.56×10^{-4}	Hobbs (1974)	α_1
	Latent heat L–ice I	kJ/kg	284	Kirk and Stevenson (1987)	L_1
	Heat capacity	J/kg/K	1925	Kirk and Stevenson (1987)	C_{p_1}
	Viscosity coefficient	Pa s	10^{12}	Grasset and Sotin (1996)	μ_0
	Activation energy	kJ/mol	*61*	Kirby et al. (1985)	Q
	Coefficient *Nu–Ra*	None	3.8	Deschamps and Sotin (2000)	a
	Coefficient *Nu–Ra*	None	0.258	Deschamps and Sotin (2000)	β
	Coefficient *Nu–Ra*	None	1.63	Deschamps and Sotin (2000)	c
Liquid layer	Density	kg/m^3	1000		ρ_2
	Expansion coefficient	K^{-1}	3×10^{-4}	Hill (1962)	α_2
	Heat capacity	J/kg/K	4180	Kirk and Stevenson (1987)	C_{p_2}
HP ices	Density	kg/m^3	1310	Hobbs (1974)	ρ_3
	Heat conductivity	W/m/K	0.56	Hobbs (1974)	k_3
	Latent heat L–VI	kJ/kg	294	Kirk and Stevenson (1987)	L_3
Silicates	Density	kg/m^3	3300		ρ_4
	Heat capacity	J/kg/K	920	Kirk and Stevenson (1987)	C_{p_4}
	Thermal diffusivity	m^2/s	1.0×10^{-6}	Hobbs (1974)	κ_4
	Half period	s^{-1}	1.38×10^{-17}		λ
	Volumetric heating	W/kg	3.18×10^{-11}		H_0
	Expansion coefficient	K^{-1}	2.4×10^{-5}	Kirk and Stevenson (1987)	α_4
	Viscosity coefficient	Pa s	1.7×10^{13}	Kirk and Stevenson (1987)	μ_4^0
	Viscosity coefficient		29.4	Kirk and Stevenson (1987)	A_4
	Viscosity coefficient	K	2300	Kirk and Stevenson (1987)	T_4^0
	Surface temperature	K	300		T_4
Iron	Density	kg/m^3	8000		ρ_5
	Melting temperature	K	1100	Urakawa et al. (1987)	T_5^0
	Temperature gradient	K/GPa	6	Urakawa et al. (1987)	b
	Latent heat	kJ/kg	570	Poirier and Shankland (1993)	L_5
	Mass fraction	%	30		x_0

wonder whether the temperature is high enough for sub-solidus convection to occur.

2.2.2. Convection in the silicate core

Initiation of convection in the silicate core has been proposed by Kirk and Stevenson (1987) for Ganymede and by Lunine and Stevenson (1987) for Titan. Using a Rayleigh number based on the boundary layer thickness, they argue that convection begins only 0.5 Ga after the core overturn. Once convection starts, they suggest that all the heat produced by radiogenic decay is expelled to the overlaying icy layers. The temperature in the core cannot increase any more and a homogeneous silicate core is always present in icy satellites. This approach does not take into account the fact that silicates have a strongly temperature-dependent viscosity. Since the silicate core is volumetrically heated [Eq. (1)] and cooled from above (icy mantle), the viscosity contrast in the upper thermal boundary layer must be very large. A conductive lid must form at the top of the silicate core and heat transfer is weaker than for the constant viscosity case.

Many experimental works and numerical studies have shown that convective motions for strongly temperature-dependent viscosity fluids are located in the part of the system where viscosity contrasts are almost negligible (e.g. Solomatov, 1995). Then, convection must be located below the thermal boundary layer in a sphere with a radius roughly estimated as follows:

$$r \approx r_4 - \sqrt{\kappa_4 (t - t_0)}. \tag{2}$$

Vigor of convection can be estimated using a Rayleigh number based on the convecting part of the system (Richter et al., 1983; Grasset and Parmentier, 1998). For a sphere of radius r, the Rayleigh number is (Weber and Machetel, 1992):

$$Ra_4 = \frac{\alpha_4 \rho_4 g H_0 \, e^{-\lambda t} r^5}{6 C_{p_4} \kappa_4^2 \mu_4(T)} \tag{3}$$

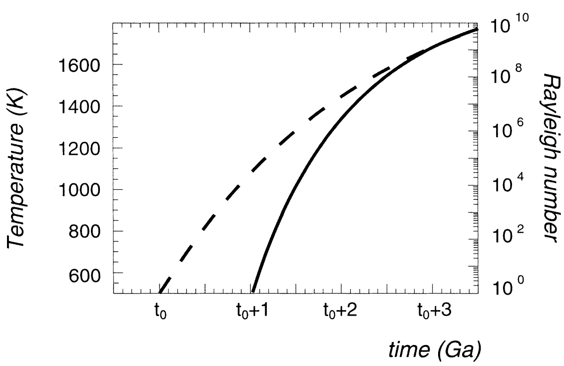

Fig. 3. Temperature (dashed line) and Rayleigh number (plain line) of the chondritic core (CI chondrites) vs time in the diffusive stage for an initial temperature of 500 K.

with parameters described in Table 1 except T, the volumetrically averaged temperature in the convecting part of the core. For a constant viscosity fluid, the critical Rayleigh number above which convection occurs depends on initial conditions, but is roughly around 2000 (Weber and Machetel, 1992). The viscosity of silicates is given by the rheological law (Kirk and Stevenson, 1987):

$$\mu_4 = \mu_4^0 \, \exp\left(A_4 \left(\frac{T_4^0}{T} - 1 \right) \right) \tag{4}$$

with μ_4^0, A_4, and T_4^0 described in Table 1. The Rayleigh number Ra_4 can be computed at each time by incorporating (1), (2) and (4) into (3). Results are plotted in Fig. 3 with $T(t_0) = 500$ K. The Rayleigh number becomes larger than 2000 at $t_0 + 1.4$ Ga (1.4 Ga after the core overturn). The temperature in the core is then equal to 1250 K. Convection is marginal and cannot evacuate all the heat produced by radiogenic decay.

In order to estimate the temperature at which a thermal equilibrium occurs, we propose the following method. Let δ, T_4, ΔT_e, and $\Delta T_c = T - \Delta T_e - T_4$ be the thickness of the conductive lid at the top of the core, the temperature at the surface of the core, the temperature drop in the convecting core, and the temperature drop in the conductive lid, respectively. ΔT_e is well defined by the relation (Davaille and Jaupart, 1993; Grasset and Parmentier, 1998):

$$\Delta T_e = -2.23 \frac{\mu(T)}{(d\mu / dT)_T}. \tag{5}$$

If there is a thermal equilibrium, the heat flux through the upper thermal boundary layer must equal the heating rate due to radiogenic decay:

$$\frac{k_4 \Delta T_c}{\delta} = \frac{\rho_4 H r_4}{3}. \tag{6}$$

Furthermore, in a well-convecting layer, the local Rayleigh number must be close to 100 (Sotin and Labrosse, 1999):

$$Ra_\delta = \frac{\alpha_4 \rho_4 g \Delta T \delta^3}{\kappa \mu(T)} \approx 100. \tag{7}$$

Combining conditions (6) and (7) with the parameters defined in Table 1 and the value of H taken at 2 Ga, we find that an equilibrium is possible for an averaged temperature in the core of 1490 K. The thickness of the lid is then roughly $\delta = 120$ km. With these conditions, it appears that convection in the core of Titan cannot be vigorous before $t_0 + 2$ Ga (Fig. 3).

The viscosity of silicates is not well constrained. The parameters proposed by Kirk and Stevenson (1987) for Eq. (4) provide a very low estimate. With these values

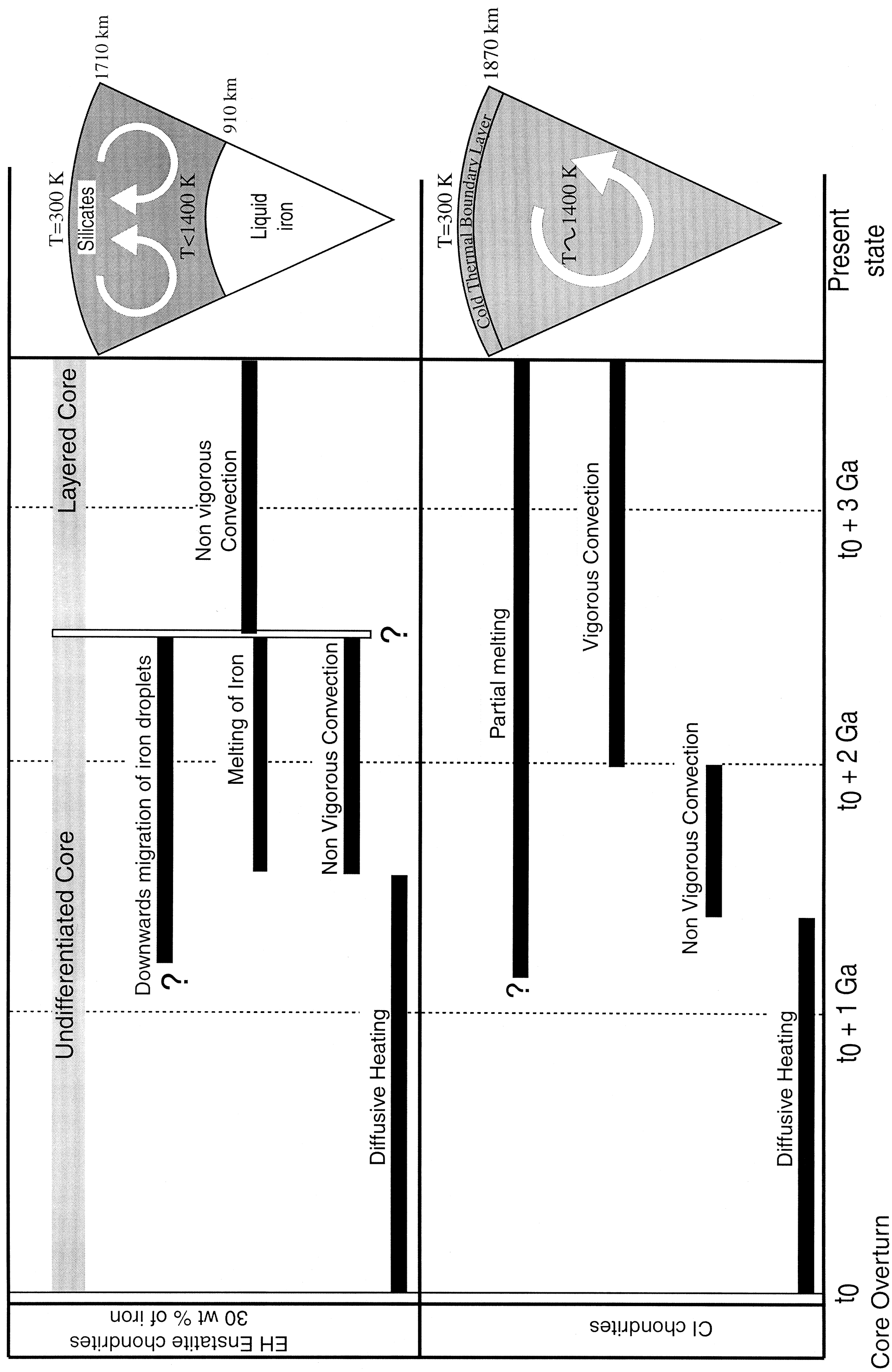

Fig. 4. The possible evolution of the chondritic core of Titan. Dark boxes indicate the duration of the different events occurring in the core.

(see Table 1), viscosity is equal to 3.6×10^{18} Pa s at 1350°C. This viscosity is 270 times lower than the viscosity generally assumed for the Earth at the same temperature (10^{21} Pa s). Because pressure and stresses on the Earth are very large, the viscosity at a given temperature must be higher than the viscosity at the same temperature on Titan. That is why we keep the parameters proposed by Kirk and Stevenson (1987). But it is worth noting that this choice provides a very low value of the viscosity of silicates. It is then possible that vigorous convection does not exist in the silicate core. For example, for a viscosity 100 times larger, marginal convection starts 1.8 Ga after the core overturn and a temperature of 1640 K is required for having thermal equilibrium. Conductive lid thickness is then equal to 138 km. Such a high temperature cannot be reached in the core before t_0+3 Ga (500 million years ago).

Despite big uncertainties about the dates proposed for the different events of the core history (mainly due to our poor knowledge of both the viscosity of silicates and the initial thermal profile in the core), the evolution of the silicate core and its present state can be roughly sketched (Fig. 4). Time duration of the different events is plotted for a cold initial thermal profile equal to 500 K.

2.3. The EH enstatite chondrite case

2.3.1. Diffusive heating

In this section, thermal evolution of an EH enstatite chondritic core with an initial amount of iron $x_0=30$ wt.% is studied. EH enstatite chondrites have been chosen for the non-icy part of planetoids because they can contain up to 35 wt.% iron (Wasson and Kalleymen, 1988). The density of the core is then $\rho_4'=(x_0/\rho_5 + (1-x_0)/\rho_4)^{-1}=4006$ kg/m^3 where ρ_5, ρ_4 are the density of iron and silicates, respectively (Table 1). In order to keep the global mass of Titan, the radius at the interface between the icy mantle and the chondritic core must be $r_4 \approx 1710$ km. We have chosen a cold initial isothermal profile $T(t_0)=500$ K which drops to the temperature of the overlying high pressure ices across a boundary layer of thickness $\sim\sqrt{\kappa_4 t_0}$. The temperature at the top T_4 is fixed and equal to 300 K, which is relevant to the melting temperature of ice VI at high pressure.

As described in the previous section, the thermal evolution of the chondritic core is controlled by the amount of volumetric heating. The temperature increases with time as:

$$T(t)-T(t_0)=\frac{(1-x_0)H_0}{C_{p_4}}\,\frac{e^{-\lambda t_0}-e^{-\lambda t}}{\lambda}. \tag{8}$$

In Eq. (8), the amount of radiogenic components in silicates is assumed equal to its amount in CI chondrites. Then, the rate of heating is smaller than for the CI case and the temperature increase from t_0 to t_0+1 Ga is now equal to 450 K (Fig. 5). Nonetheless, it is possible that convective motions exist. The Rayleigh number of the whole sphere is now equal to:

$$Ra_4=\frac{\alpha_4\rho_4' g(1-x_0)H_0\, e^{-\lambda t} r^5}{6C_{p_4}\kappa_4^2\mu_4(T)} \tag{9}$$

where r is given by Eq. (2) and $\mu_4(T)$ is still given by Eq. (4).

The Rayleigh number Ra_4 can be computed each time using Eqs. (2), (4), (8) and (9). The temperature in the core and the Rayleigh number are plotted in Fig. 5. Two billion years after the core overturn, the temperature is almost equal to 1200 K and higher than the melting temperature of iron (see Section 2.3.2). Nonetheless, the Rayleigh number is still very small (around 20). Results presented in Fig. 5 indicate that the melting of iron probably occurs because the heat cannot be expelled by convection. This result does not depend on the choice of an initial thermal profile. Changing the initial temperature only implies a variation of the time needed for starting the melting of iron. This time varies from $t_0+2.3$ to $t_0+0.7$ Ga for an initial temperature of 400 and 800 K, respectively. However, results may depend strongly on the viscosity law chosen. We have assumed that the viscosity of the system silicates–iron is equal to the viscosity of pure silicates. If the viscosity is larger, then melting will almost surely occur during the first billion years. If the viscosity is smaller, convective motions may start before the melting of iron if, at the melting temperature of iron, the Rayleigh number Ra_4 is higher than the critical Rayleigh number. Viscosity must be at least two orders-of-magnitude lower than the value pro-

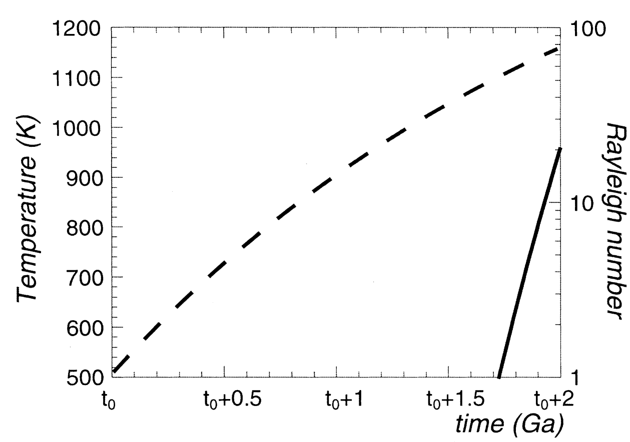

Fig. 5. Temperature (dashed line) and Rayleigh number (plain line) of the chondritic core (EH Enstatite chondrites) vs time in the diffusive stage for an initial temperature of 500 K.

posed in Eq. (4) which is itself an underestimate of the viscosity of silicates (see Section 2.2.2). Such a low value is highly unrealistic. The melting of iron probably occurs before the onset of convection in Titan's core.

2.3.2. Melting of iron

Since the initial chondritic core cannot efficiently evacuate the radiogenic heat produced in silicates at a temperature close to the melting temperature of iron, the core must differentiate into a liquid iron inner core surrounded by an iron depleted silicate mantle. In order to investigate this process, we have set up a diffusive model where the temperature in the core is computed each time using the diffusion equation:

$$\frac{\partial T}{\partial t} = \kappa_4 \nabla^2 T + (1 - x_0)\frac{H_0}{\rho_4' C_{p_4}} e^{-\lambda t}. \tag{10}$$

All the parameters are described in Table 1. Eq. (10) is solved using a Crank–Nicholson scheme. Each time and for all depths, the temperature is compared to the eutectic temperature in the system Fe–Ni–O–S:

$$T_m^5(P) = T_5^0 + b \cdot P \tag{11}$$

where T_5^0 is the eutectic temperature at ambient pressure, P is the pressure and b the temperature gradient. The melting temperature of an iron-rich system depends strongly on its chemical composition. For example, the melting temperature of pure iron at 160 kbar is around 2200 K. If sulfur or oxygen are present, the binary systems Fe–FeS or Fe–FeO start to melt at 1650 K (Boehler, 1992). At low pressures (5–15 GPa), Urakawa et al. (1987) have shown that the eutectic temperature in the system Fe–Ni–O–S is around 1100 K. Since iron cannot be pure in chondrites, we have used experimental data proposed by Urakawa et al. (1987) in the system Fe–Ni–O–S for prescribing the constants T_5^0 and b (see Table 1). When the temperature at depth becomes equal to the eutectic temperature of iron, the heat provided by radiogenic decay is used for melting:

$$\frac{dx}{dt} = (1 - x_0)\frac{H_0 e^{-\lambda t}}{L_5} \tag{12}$$

where x is the fraction of iron that is melted at time t. Once iron is melted, the temperature increases again by diffusion.

The evolution of the temperature with time has been plotted in Fig. 6 for $T(t_0) = 500$ K. Temperature profiles are plotted for different times and compared to the melting temperature of iron (bold line). The temperature increases up to the melting temperature 1.6 Ga after the core overturn. Less than 1 Ga later, most of the iron of the deepest part of the core is melted, but due to the cooling from the top, the melting of the 510-km thick outer thermal boundary layer is very difficult. Melting occurs mainly in the deeper part of the core (1/3 of its volume).

Since iron is denser than silicates, it must fall towards the center of Titan. A simple Stockes model cannot estimate the time required for this overturn because the droplets of iron probably move inwards along the grain boundaries of silicates. More complicated models are then required, but are out of the goal of this paper. Since the recent magnetic data and gravity data of Galileo suggest that a deep metallic liquid core exists on Ganymede (Kivelson et al., 1996; Anderson et al., 1996; Stevenson, 1996), let us assume that the formation of an iron core also occurred on Titan. This assumption will have to be tested by the Cassini mission. During the diffusive heating of the chondritic core, a small part of the metallic iron is melted in the deepest part of the core (Fig. 6). This process is very slow (1.5 Ga for an initial thermal profile of 500 K) so that inward migration of solid iron along grain boundaries probably occurs in the meantime and is followed by melting as the iron goes down. Furthermore, during the heating of the core by radiogenic decay (Fig. 5), the viscosity of chondrite decreases and convective motions could start. Convective motions accelerate the formation of a layered core because iron droplets migrate easily downwards into cold plumes, but cannot migrate upwards along hot plumes (hot plumes do not exist when a fluid is volumetrically heated and the density difference between iron and silicate impedes the

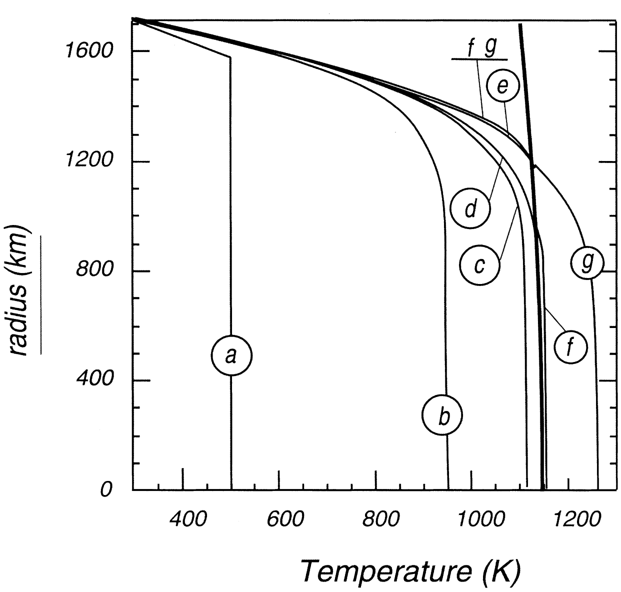

Fig. 6. Temperature in the chondritic core as a function of depth for different times: (a) $t_0 = 1$ Ga; (b) $t_0 + 1$ Ga; (c) $t_0 + 1.5$ Ga; (d) $t_0 + 1.6$ Ga; (e) $t_0 + 2.4$ Ga; (f) $t_0 + 2.5$ Ga; and (g) $t_0 + 3.0$ Ga. Two billion years after the core overturn, the temperature in the deep core becomes higher than the melting temperature of iron (bold line).

iron to migrate upward). Except for the upper part of the cold thermal boundary layer of the chondritic core (Fig. 6) which is possibly too viscous to be incorporated in convective motions, most of the iron trapped initially in the thermal boundary layer of the chondritic core go down and melt. Finally, for $x_0 = 30$ wt.% and if we neglect the small amount of iron which could be trapped below the icy mantle, a layered structure composed of a 910 km iron liquid core and a 800 km thick silicate outer shell occurs (Fig. 4).

2.3.3. Convection in the silicate layer

The new silicate outer shell is overlain by a cold icy shell ($T_4 = 300$ K). It is heated both from within and from below since the melting temperature of the iron core fixes the temperature at the bottom. The temperature drop at the top of the layer is large and convection must be located in the deeper part under a stagnant lid where most of the viscosity contrast occurs. In this stagnant lid regime, convective motions are well described using parameterized laws of thermal convection for constant viscosity fluid with a proper parameterization (Davaille and Jaupart, 1993; Grasset and Parmentier, 1998; Choblet et al., 1999). Convection is possible if the Rayleigh number calculated with the viscosity at the volumetrically averaged temperature of the layer:

$$Ra = \frac{\alpha_4 \rho_4 g(\bar{T} - T_4)(r_4 - r_5)^3}{\kappa_4 \mu_4^0 \, \exp\left(A_4\left(\dfrac{T_4^0}{\bar{T}} - 1\right)\right)} \tag{13}$$

is larger than the critical Rayleigh number defined for a constant viscosity fluid (roughly 1000). In (13), r_4, r_5 are radii at the top and bottom of the silicate layer, respectively, $\bar{T}$ is the volumetrically averaged temperature, and all the other parameters are defined in Table 1. If the average temperature in silicates is fixed to 1300 K in Eq. (13), the Rayleigh number is equal to the critical Rayleigh number and convection is possible. Convection becomes vigorous ($Ra > 10^5$) if the temperature is higher than 1400 K. After the melting of the iron, the temperature in the silicates was around 1100 K. During the last billion years, radiogenic decay has been weak compared to the beginning and the temperature increase is lower than 200 K. Then, the average temperature in silicates is probably lower than 1400 K and convective motions, if they exist, are weak. In addition, the iron core must be totally liquid because the heat cannot be expelled efficiently through the silicate layer.

The evolution of the chondritic core of Titan has been summarized in Fig. 4. Black boxes indicate the duration of every event. Question marks indicate the events for which we have no information about duration or date.

2.4. The heat flux at the surface of the core

In the previous sections, it has been shown that convection in Titan's core is very probable, but is not necessarily vigorous. The heat flux at the surface of the core must be higher than the conductive heat flux, but lower or equal to the convective heat flux obtained assuming that convection is sufficiently vigorous for expelling all the heat produced by radiogenic decay:

$$F_4^{\mathrm{t}} = \frac{\rho_4 (r_4^3 - r_5^3)}{3 r_4^2} H_0 \, \mathrm{e}^{-\lambda t}. \tag{14}$$

One could argue that, if convection is vigorous, Eq. (14) could underestimate the heat flux. For example, on Earth, where convective motions are very vigorous, geochemical data indicate that the present ratio of heat generation versus heat output must be in the range 25–58% (e.g. Christensen, 1985). A classic scenario of accretion can explain this very small ratio. During accretion, the amount of energy that is transformed into heat is tremendous. Just after accretion, the inner part of the Earth is cold but the outer silicate shell is very hot and probably partially molten. The formation of the core is rapid and leads to an inversion of the thermal profile. Because the temperature is very high, very vigorous subsolidus convection starts in the silicate layer immediately after the core overturn. Both the heat trapped after accretion and the heat produced by radiogenic decay are expelled from the convecting mantle. The amount of heat trapped initially in the outer shells during accretion and dissipated in the interior during the core formation was so important that it is still expelled from the mantle.

In icy satellites, the amount of heat stored during accretion is much smaller. Furthermore, the temperature in silicates does not increase very much because the melting of ices provides an efficient temperature buffer during accretion. The core overturn still implies an inversion of the temperature profile, but the amount of heat dissipated during this overturn is very small. As was explained in Section 2.2.1, the temperature of the chondrites trapped in the core is probably lower than 600 K after the overturn. Radiogenic decay will then increase the temperature up to a critical value where convection can start. In that case, convective motions can expel the heat produced by radiogenic decay, but because there are no other sources, the heat flux cannot be significantly larger than the heat flux proposed in Eq. (14).

The heat flux at the surface of the core could also be larger than the value proposed in Eq. (14) because of the cooling of the iron inner core. Taking the parameters in Table 1, the cooling of the iron sphere from 1400 to 1100 K (which is probably the highest possible temperature drop in the liquid core) during the last billion years increases the heat flux F_4^t by less than 1%. Then, we argue that Eq. (14) provides a good estimate of the highest heat flux which can escape from the core.

2.5. The present internal structure of Titan's core

In Sections 2.2 and 2.3, it has been shown that the internal structure of Titan's core depends strongly on the amount of metallic iron included in planetoids (Fig. 4). At present, Titan's core is either a well-convecting silicate sphere (CI chondrites case) or a layered structure composed of a liquid iron inner core surrounded by a slowly convecting silicate layer (EH enstatite chondrites). The volume of the iron core relative to the silicate layer depends on the initial amount of metallic iron in chondrites. The Cassini orbiter will probably provide the structure of the core.

In the two extreme cases presented, both a low temperature compared to terrestrial planets (lower than 1400 K) and a very stable structure characterize the core. Indeed, once vigorous convective motions have started in the core, no further important evolution is possible. This arises from the strong buffering effect of convective motions (Tozer, 1972). A temperature increase (decrease) implies more (less) vigorous convection because the viscosity decreases (increases). This change in the vigor of convection acts against its cause and the system is actually fully regulated.

Another possible evolution of the core relative to the structure proposed in Fig. 4 could be the crystallization of the iron inner core for the EH enstatite chondrites case. But this crystallization is only possible if the temperature at the interface between the iron core and the silicates decreases down to 1200 K [Eq. (11)]. It is actually impossible to have such a low value because of the radiogenic heating. Then, if the iron core of Titan exists, it must be liquid.

3. The internal structure of the icy mantle

The icy layer of Titan was formed very early in the history of the satellite. It is composed of water and probably many volatiles, which were incorporated in planetoids during accretion. This icy layer can be composed of several sublayers because the range of pressure encountered from the surface to the top of the core allows the existence of several high-pressure polymorphs of ice. Furthermore, a deep liquid layer could exist below an ice I outer layer. The purpose of this section is to discuss the present state of the icy mantle of Titan.

3.1. The pure water case

The simplest case arises from the assumption that Titan is composed of pure water and chondrites. The effects of other components will be described in Section 3.2. Grasset and Sotin (1996) have shown that the freezing of a primordial pure water liquid layer was very fast and completed before the core overturn. At the time t_0, Titan was composed of a chondritic core surrounded by a thick solid icy layer (Fig. 2(a)). Due to the low temperature at the surface, the icy mantle must be split into a conductive lithosphere at the top and a convecting mantle below. Convective motions in the icy layer are very complex because several high-pressure phases can be present. Bercovici et al. (1986) and Sotin and Parmentier (1989) have shown that exothermic phase changes can either impede or enhance whole-layer convection and that endothermic phase transition are a barrier to whole layer convection and may result in leaky two-layer convection. Forni et al. (1998) have established that the transition II–VI is a strong barrier against whole-layer convection and that a two-layered convection is probable in large icy satellites like Titan. All these studies show clearly that it is difficult to describe accurately the convective motions in a whole icy layer. Nonetheless, the important result is that convective motions are always very vigorous (Coradini et al., 1995) and provide an efficient means to expel all the heat produced in the core. If Titan were composed of pure water and chondrites, the icy mantle would now be completely frozen and would convect strongly. We do not believe that this model is a plausible one. A recent review (Kargel, 1998) shows well that many components like ammonia hydrates and salts must have been incorporated in ices before the accretion of the satellites. The effect of these components is studied in the following section by taking the example of ammonia.

3.2. The rich volatiles case

3.2.1. The influence of ammonia

If volatiles are incorporated in ices during the accretion of Titan, the freezing temperature of the liquid layer can be decreased compared to the pure water case. The example of ammonia has been chosen because solid ammonia–water compounds may have condensed during the formation of Titan (Yarger et al., 1993). Furthermore, the phase diagram of the NH_3–H_2O system at low temperature is well known both at low pressures (Rollet and Vuillard, 1956; Kargel, 1992; Hogenboom et al., 1997) and high pressures (Johnson and Nicol, 1987; Boone and Nicol, 1991; Grasset et al., 1995; Hogenboom et al., 1997). Based on all these experimental results, a plausible T–P–X phase diagram in the water rich region of the ammo-

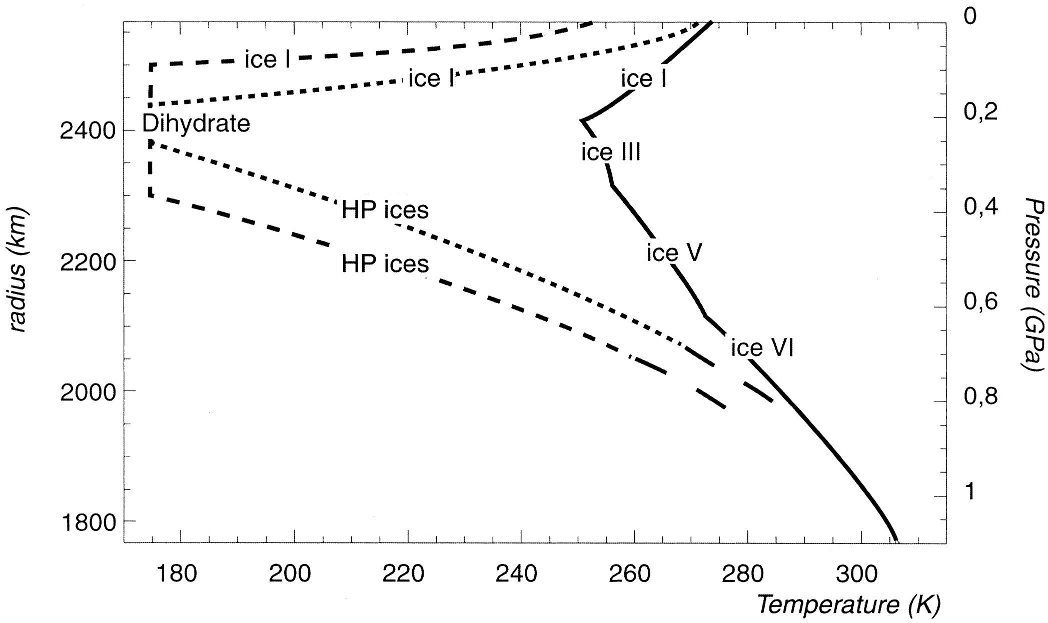

Fig. 7. Liquidus curves for different composition of the liquid layer: pure water (plain line), 5% ammonia (dotted line), 15% ammonia (dashed line).

nia–water system has been proposed (Sotin et al., 1998). At low pressures, the liquidus curve of the temperature–composition phase diagram varies from 273 K (melting temperature of pure water) to 177 K (melting temperature of the eutectic composition). For higher pressures, the melting temperature of water decreases, but the melting temperature of the eutectic is almost unchanged. For any temperature between the liquidus temperature and the solidus temperature, an ammonia rich liquid coexists with pure ice. If the temperature decreases below the solidus (177 K), a complete crystallization is achieved and two solids coexist: ammonia dihydrate and water ice. Eventually, the ammonia dihydrate can be replaced by high-pressure polymorphs (Hogenboom et al., 1997).

Using these experimental data, liquidus curves have been computed for both an NH_3 (15%)–H_2O (85%) and an NH_3 (5%)–H_2O (95%) primordial ocean (Fig. 7). The parameters that describe these liquidus are indicated in Table 2a. The melting curve of water (Chizhov, 1993) has also been plotted for comparison. Depending on the radius of the core, the position of the boundaries between ices and ammonia dihydrate might change slightly. But this change is very small and will be neglected.

3.2.2. Transfer of heat through the ice I shell

Grasset and Sotin (1996), using an isoviscous scaling law and an isothermal criterion for describing the transition between the conductive lid near the surface and the convecting ice, have shown that the presence of ammonia impedes the complete crystallization of the liquid layer after the primordial core overturn. It is probable that, after the formation of an iron core (EH enstatite chondrites case) or the onset of vigorous convection in the silicate core (CI chondrites case), a thick liquid layer still exists on Titan. The satellite is composed of a deep high-pressure icy layer over the core, surrounded by a liquid shell and an ice I cap (Fig. 2(b)). In this section, scaling laws for strongly temperature-dependent fluids are used for describing how the heat can be expelled through the ice I cap.

Heat flux through a convecting layer is generally derived from a simple scaling law which relates the vigor

Table 2a
Singular points on the liquidus curves

	NH_3 (5%)–H_2O (95%)			NH_3 (15%)–H_2O (85%)		
	Radius (km)	*P* (GPa)	*T* (K)	Radius (km)	*P* (GPa)	*T* (K)
Surface	2575	0	271.6	2575	0	253
Ice I–dihydrate interface	2449	0.17	176	2508	0.09	175
Dihydrate–HP ices interface	2375	0.27	178	2300	0.38	180

of convection (Rayleigh number) to the heat flux (Turcotte and Schubert, 1983):

$$F_1^b = k_1 \frac{T(r_2) - T(r_1)}{r_1 - r_2} a\, Ra^{\beta} \tag{15}$$

where a and β are coefficients. When the fluid has a viscosity that is strongly temperature-dependent, the flow pattern and the efficiency of the heat transfer differ strongly from the constant viscosity case. Experimental (Booker, 1976; Nataf and Richter, 1982; Richter et al., 1983) and numerical (Christensen, 1984; Moresi and Solomatov, 1995) studies have shown that a quasi-stagnant lid develops at the top and that convective motions occur underneath where the viscosity contrasts are very small. Christensen (1984) pointed out that Eq. (15) is not valid in that case. Morris and Canright (1984) suggested that the heat flux can be determined as a function of both the internal Rayleigh number defined with the viscosity in the well-mixed interior and an additional parameter γ which describes the amplitude of the viscosity contrasts. The parameter γ is defined by the following equation:

$$\gamma = \frac{T(r_2) - T(r_1)}{\Delta T_v} \tag{16}$$

with

$$\Delta T_v = -\frac{\mu_1(\bar{T})}{(\mathrm{d}\mu_1/\mathrm{d}T)_{\bar{T}}} \tag{17}$$

where $\bar{T}$ is the volumetrically averaged temperature in the convecting layer and μ_1 is the viscosity of ice I. The heat flux at the bottom of ice I is then accurately defined by:

$$F_1^b = k_1 \frac{T(r_2) - T(r_1)}{r_1 - r_2} a\, Ra^{\beta}\, \gamma^c \tag{18}$$

where

$$Ra = \frac{\alpha_1 \rho_1 g (T(r_2) - T(r_1))(r_1 - r_2)^3}{\kappa_1 \mu_1(\bar{T})}. \tag{19}$$

The parameters a, β, and c used in (18) have been computed by Moresi and Solomatov (1995) and Deschamps and Sotin (2000). They found comparable but slightly different values. The most recent values proposed by Deschamps and Sotin have been preferred: $a = 3.8$, $\beta = 0.258$ and $c = 1.63$.

The viscosity of ice I is strongly temperature-dependent and to a lesser extent pressure-dependent (e.g. Goodman et al., 1981; Weertman, 1983; Goldsby and Kolhstedt, 1997). Weertman (1983) has proposed a simple relation where the pressure dependence appears implicitly:

$$\mu_1(\bar{T}) = \mu_0\ \exp\left(\frac{Q}{RT_m}\left(\frac{T_m}{\bar{T}} - 1\right)\right) \tag{20}$$

with T_m the melting temperature of water ice, μ_0 the reference viscosity, Q the activation energy and R the gas constant. T_m is given by the melting curve of water ice and varies with depth. It then accounts for the pressure dependence of viscosity. For the sake of simplicity, the pressure dependence of the viscosity is neglected by fixing $T_m = 260$ K. The reference viscosity μ_0 is deduced from measurements of glacier flow (Gerrard et al., 1952).

Finally, theoretical works (Morris and Canright, 1984) predict that the temperature drop in the bottom thermal boundary layer must be proportional to ΔT_v:

$$\bar{T} - T(r_2) = d \cdot \Delta T_v \tag{21}$$

with the coefficient d close to one. Numerical results of Deschamps and Sotin (2000) suggest a slightly different coefficient (d = 1.43) which has been preferred. Incorporating (20) into (17) allows us to compute ΔT_v as a function of $\bar{T}$. Eq. (21) is then reduced to a second-order polynomial which admits only one positive solution:

$$\bar{T} = \frac{Q}{2Rd}\left[\sqrt{1 + \frac{4Rd}{Q} T(r_2)} - 1\right]. \tag{22}$$

By introducing (22), (20), and (19) into (18), the heat flux F_1^b depends only on the melting temperature of ice $T(r_2)$ at the interface between the ice I shell and the liquid layer. The temperature $T(r_2)$ being defined by a second-order polynomial (Table 2b), Eq. (18) is actually a relation between the heat flux F_1^b through the ice I layer and the radius r_2 at the bottom of the layer.

The amount of heat expelled per unit time in the ice I layer has been plotted as a function of the thickness of the ice I layer ($r_1 - r_2$) in Fig. 8. Values are given relative to the highest global heat flux expelled from the core computed for $t = t_0 + 1.6$ Ga (onset of vigorous convection). Three curves have been plotted depending on the amount of ammonia. The shaded area represents the possible domain of the global heat flux from the core. The lowest value corresponds to the present global heat flux if there is no convection in the core. As long as the curves are above the shaded

Table 2b
Liquidus coefficients: $T_m(P) = a_0 + a_1 P + a_2 P^2$

% NH_3	Phase	a_2 (K/GPa^2)	a_1 (K/GPa)	a_0 (K)
5	I	−2824	−79.4	271.6
	HP ices	−152.9	363.7	91.0
15	I	−8634	−85.1	253.0
	HP ices	−215.5	479.8	28.5

area, there is more heat expelled through the ice I layer than heat produced in the core by radiogenic decay and crystallization of the liquid layer must occur. In the pure water case (curve 1), the global heat flux through the ice I shell is always larger than the global heat flux from the core which confirms that a rapid crystallization of the liquid layer occurs. When ammonia is present, the evolution is different because the global heat flux through the ice I shell crosses the shaded area. At the beginning, there must be a rapid thickening of the ice I shell but very rapidly, heat transferred through the ice I shell becomes almost equal to the heat expelled from the core. A thermal equilibrium is then reached. The evolution of the internal structure is then very slow and is imposed by the decrease of the amount of heat expelled from the core [see Eq. (14)]. For 5% of ammonia, the present thickness of the ice I shell must be close to 80 km. For 15% of ammonia, the thickness of the icy layer is less than 40 km.

3.2.3. The internal structure of the icy mantle

It has been shown in the previous section that a thermal equilibrium is achieved very rapidly when volatiles are incorporated in the liquid layer. In this section, some properties of thermal equilibrium will be used for providing a good description of the different layers of Titan. We assume that all the heat is provided from the core and that the solid tidal dissipation rate can be neglected. Indeed, Sohl et al. (1995) have shown that the interior tidal heating is more than 10 times lower than the radiogenic heating.

At each time, the heat flux at the bottom of the ice I layer F_1^b must equal the heat flux from the liquid layer F_2^t (Fig. 2(b)):

$$F_1^b = F_2^t. \tag{23}$$

The total heat flux at the top of the liquid layer differs very slightly from the total heat flux from the core because melting can occur at the bottom of the high pressure icy layer (Grasset and Sotin, 1996). This small discrepancy is actually very small and can be neglected. A simple relation can then give the heat flux in the liquid layer F_2^t from the heat flux from the core F_4^t:

$$F_2^t = \frac{r_4^2}{r_2^2} F_4^t. \tag{24}$$

The introduction of Eqs. (24) and (18) into (23) provides a relation between r_2 and F_4^t which can be solved by successive iterations. For a given heat flux at the top of the core, Eq. (23) then provides the internal structure of the icy layers of Titan. The radius of the bottom of the liquid layer r_3 (see Fig. 2) can be found by assuming that the thermal profile in the liquid layer is adiabatic (Grasset and Sotin, 1996).

Eq. (23) has been solved for several values of the heat flux from the core and for two different compositions of the primordial liquid layer. Results are plotted in Fig. 9 for two initial amounts of NH_3 (5 and 15%). Once r_2 is found, the thickness of the ice I layer is given by the difference $r_1 - r_2$, and the thickness of the conductive lid is computed using the Fourier law:

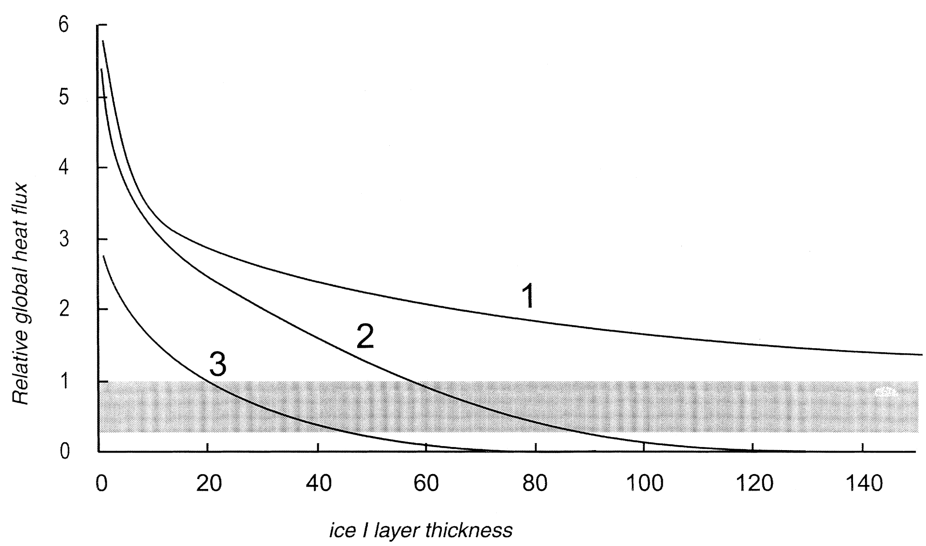

Fig. 8. Global heat flux vs thickness of the ice I layer. Heat flux is given relative to the highest global heat flux from the core. The shaded area represents the possible range of the relative global heat flux from the core. Three cases are presented: (1) pure water; (2) 5% ammonia; and (3) 15% ammonia.

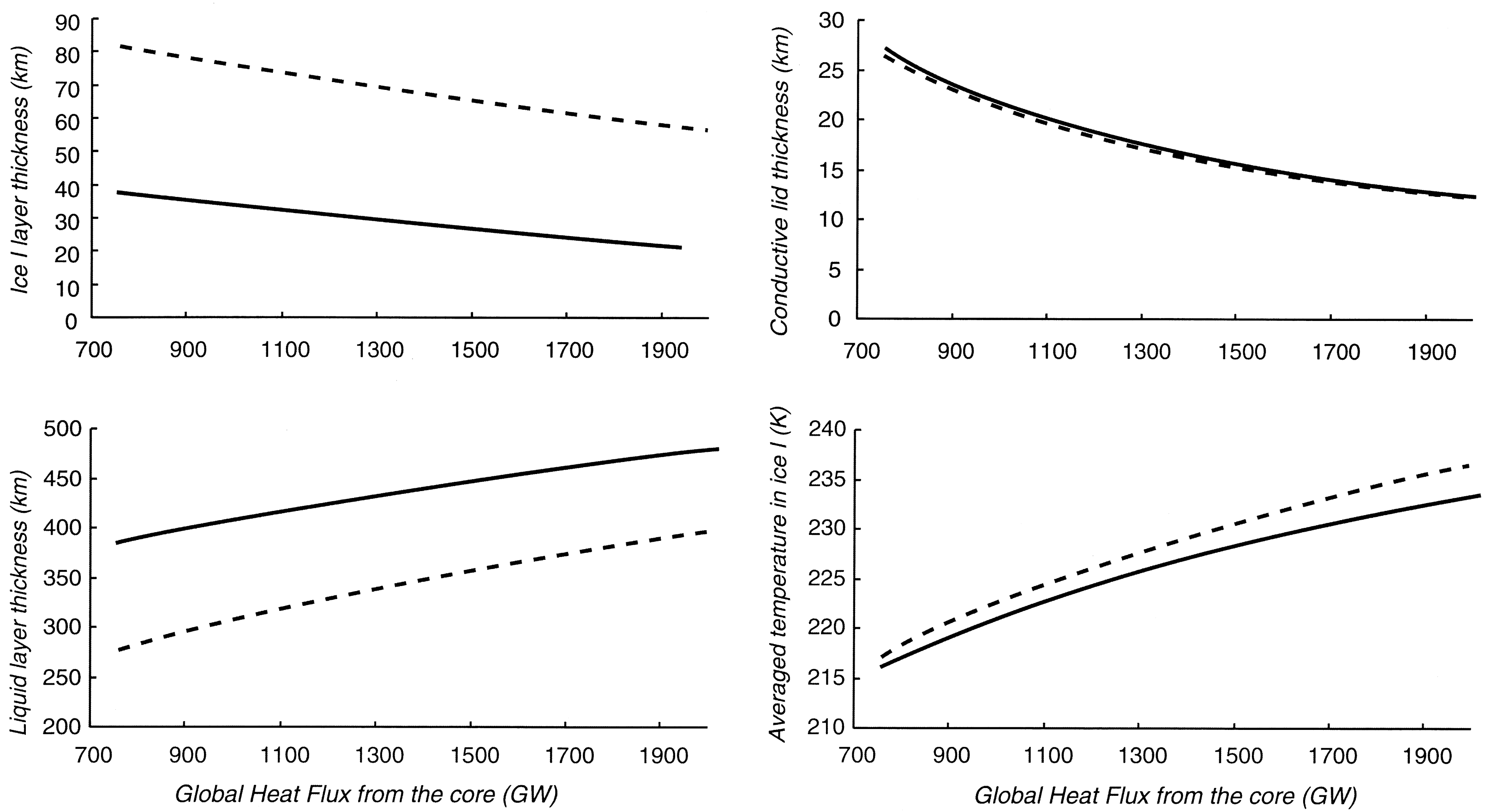

Fig. 9. Internal structure of the icy mantle of Titan as a function of the global heat flow expelled from the core for two distinct amounts of ammonia: dashed lines, 5%; plain lines, 15%. A global heat flux of 1.9 TW corresponds to the highest possible energy that can be expelled per unit time by the core once vigorous convection has started. At present, the heat flow is smaller and probably around 0.7 TW.

$$\delta = \frac{r_1^2}{r_2^2}\frac{k_1(\bar{T} - T(r_1))}{F_1^{\mathrm{b}}} \tag{25}$$

assuming that the global heat flux at the top of ice I is equal to the global heat flux at the bottom, the liquid layer thickness is the difference r_2–r_3, and the average temperature in the ice I layer is given by Eq. (22). These data characterize the internal structure of the icy layers of Titan if there is a thermal equilibrium. The lowest value of the global heat flux from the core (0.7 TW) corresponds to a plausible present value if convective motions are vigorous in the silicates (see Sections 2.2.2 and 2.3.3). The increase of the global heat flux from 0.7 to 1.9 TW corresponds to a motion backward in time. The value 1.9 TW is roughly the highest heat flux that can be expelled from the core when convection is vigorous (2 Ga ago). The main result is that the crystallization of the liquid layer on Titan is not possible if ammonia is present. Even with an initial amount of 5%, there must still be a liquid layer 280-km thick. Its thickness increases with the initial amount of ammonia and can be as large as 380 km if 15% of ammonia were included in planetoids. Temperature in the liquid layer is probably in the range 220–250 K. Using all these results, a possible internal structure of Titan at present has been sketched in Fig. 10. The structure of the core is drawn using the results of the second section.

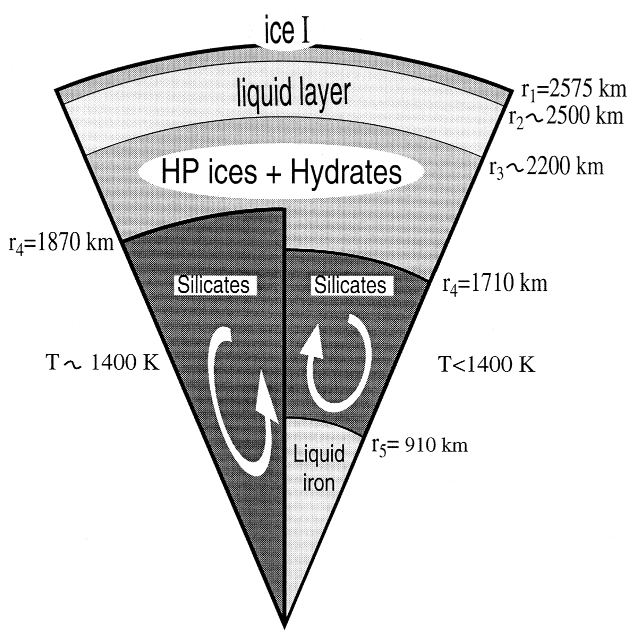

Fig. 10. A possible present internal structure of Titan.

4. Discussion

4.1. Sources of internal heating

The internal structure has been described by assuming that thermal equilibrium is achieved at each time, which means that the convective motions are sufficiently vigorous to respond rapidly to any variation of the amount of heat sources. This property of a well-convecting system has often been applied in thermal evolution models because the scaling laws used for the determination of the heat flux are always based on the numerical and experimental results obtained in systems which are in thermal equilibrium. This approach has been recently confirmed for a convecting fluid with strongly temperature-dependent viscosity by Choblet et al. (1999). The authors have shown that the cooling rate of a convecting fluid cooled from above can be predicted accurately with scaling laws that describe the stagnant lid regime for a volumetrically heated fluid.

In Titan, the possible heat sources include: (1) radiogenic decay in the core; (2) tidal heating; (3) cooling of the different shells; and (4) possible freezing of the liquid layer. The present model only takes into account radiogenic decay, which represents a lower limit for the internal heating and therefore minimizes the probability of a deep ocean to exist. In addition, the three other sources of energy are much less important than the radiogenic decay: tidal heating is more than 10 times lower than radiogenic heating (Sohl et al., 1995), a regular cooling of the whole mantle from 300 to 100 K (which is highly impossible to achieve because of the heating from the core) may represent a source of power roughly equal to a tenth of the present (and lowest) power produced by the core, and the crystallization of ice I at the top increases the internal heating by less than 3%. The addition of these amounts of heat in the model favor the existence of a liquid shell under an ice I layer.

4.2. The viscosity of ices

The results depend on the viscosity of ices because it is the heat transfer through ice I which controls the evolution of the mantle. The conductive lid thickness is almost unchanged, but the present thickness of the ice I layer decreases (increases) by 10 (8) km if the viscosity is increased (decreased) by a factor of 10. These variations do not change the main conclusion: a thick liquid layer is still present on Titan. Furthermore, we argue that the results proposed above are valid because the viscosity of ice is relatively well known. Many experiments at high stresses have been conducted and provide good estimates of the activation energy (Weertman, 1973, 1983; Kirby et al., 1985; Durham et al., 1993; Goldsby and Kolhstedt, 1997). Furthermore, viscosity measurements in glaciers (Hobbs, 1974) show that ice I must have a Newtonian behavior at geologic time scales. It is then possible to estimate with a relatively good accuracy the viscosity of ices in the range of temperature encountered in icy satellites (Grasset and Sotin, 1996).

During the last 20 years, our understanding of thermal transfer through convecting layers has been greatly improved. The fact that icy layers have a viscosity which is strongly temperature-dependent no longer impedes one to make accurate models of thermal evolution because scaling laws for variable viscosity fluids are now available (Moresi and Solomatov, 1995; Solomatov, 1995; Grasset and Parmentier, 1998; Deschamps and Sotin, 2000). Compared to previous models issued from studies on isoviscous fluids, the new parameterized laws take into account the fact that the temperature contrast in the convecting layer is defined by rheological criteria [Eqs. (17) and (21)]. It implies that the transition between the cold stagnant lid at the top and the convecting layer cannot be defined by an isotherm. Another characteristic of the stagnant lid regime is that the vigor of convection is not simply related to the averaged temperature in the mantle as was suggested by Tozer (1972), but also to the thickness of the conductive lid. It is possible to have a very vigorous convection in ice I, but a small global heat flux because the lid at the top is very thick. The example proposed above illustrates well that both the temperature of the mantle and the thickness of the lithosphere regulate the thermal evolution of Titan.

4.3. The chemical composition of the liquid layer

As it is shown in Fig. 9, the internal structure of the ice I layer does not vary very much from 2 Ga to the present because of the variation of the heat flux from the core. It is the composition of the liquid layer that is of fundamental importance. The present atmosphere of Titan indicates that the actual composition of the icy layer and the possible liquid layer is probably very complex. Methane and nitrogen could be present. Furthermore, recent data of Galileo on Europa show that salts may be present on the surface of Europa (McCord et al., 1998). Nobody knows if these salts, if they exist, could not also be present on Titan. It has been suggested that salty liquid–water oceans on Europa and Callisto could explain the induced magnetic fields observed by the Galileo spacecraft (Khurana et al., 1998). It is then possible that the Cassini orbiter will provide strong evidence for the presence or absence of salts on Titan. For understanding the influence of volatiles on the internal structure of Titan, more experimental data are required. No experimental works have been conducted for nitrogen–water and methane–water systems at high pressures and low temperature. Without these data, it is not possible to have a precise understanding of the different events occurring in the icy layers and the liquid layer of Titan.

Lunine (1993) has shown that an underground ocean is the only structure that is consistent with all of the known constraints (chemical, tidal, ground-based radar and near-infrared observations). We have shown that thermal evolution models also predict this structure when scaling laws for variable viscosity fluids are taken into account. Titan's structure proposed in Fig. 10 differs from the internal structure proposed by Lunine (1993, 1994) by two points: the liquid layer is almost 100 km thicker and the ice I layer is relatively thin (less than 80 km). These points are of great importance because Lunine and Stevenson (1987) have shown that the methane initially trapped in the primordial core cannot reach the outer icy layer if the ammonia–water liquid shell is too thick. During its ascent from the primordial core, the methane must indeed combine with liquid water to form clathrate hydrates. Since we know that methane is present at the surface or at a very shallow depth in great quantities and that the primordial methane was expelled during the first stages of Titan's history, there must be a way to transfer the methane from the liquid layer towards the surface. But the methane cannot ascend directly through the liquid layer as Lunine and Stevenson (1987) suggested. The methane trapped in the liquid layer must rather be incorporated in ices during the freezing of the ice I shell and entrained by convective motions towards the surface. Unfortunately, the exact scenario is impossible to describe because of the lack of experimental data. High-pressure and low-temperature experiments on complex mixtures of ammonia and methane are required if one wants to understand how the constant replenishment of methane at the surface of Titan is possible.

4.4. Constraints by the data which will be acquired by Cassini

The interpretation of recent Galileo data on both the magnetic field of Europa and Callisto (Khurana et al., 1998) and the geological feature of these two galilean satellites (Pappalardo et al., 1998) suggests that a deep ocean would be present within these two satellites. The presence of a deep ocean within Titan may be constrained by the Cassini mission with the help of remote sensing of the surface (radar and/or infrared), radio science for the determination of the gravity field, and magnetic field measurements. Since Titan's eccentricity is large (on the order of 3%), the non-hydrostatic component on J_2 and J_{22} may provide values of the dynamic Love numbers (k_2) if the true anomaly is different from 90° and if measurements made at different latitudes and longitudes can be carried out. It is out of the goal of the present paper to provide a detailed study of the relationship between the internal structure, the values of the Love numbers, and the gravitational coefficients. Preliminary results show that the relative accuracy on the gravity coefficients must be as good as 10^{-7} to determine the presence of a deep ocean, a value which seems compatible with the characteristics of the radio science experiment on Cassini (Rappaport et al., 1997). A forthcoming paper describing the relationships between the internal models and the gravitational coefficients will address this issue in the light of the characteristics of Tour 18-5, which has been chosen as the Cassini orbit around Saturn.

5. Conclusion

Evolution of the silicate core of Titan has been presented for two extreme compositions of chondrites. The present internal structure of Titan's core must be somewhere between these two extreme cases. If CI chondrites were included in planetoids, the present core of Titan is a homogeneous layer that convects strongly. It is characterized by a thick thermal boundary layer at the top and a well-mixed convecting layer with an average temperature around 1400 K. If chondrites were EH enstatite chondrites, Titan's core is divided into two parts: an inner liquid iron core surrounded by a well-convecting silicate layer. The crystallization of this liquid iron seems impossible because convective motions in the silicate layer are not vigorous. The Cassini orbiter will probably provide the exact structure of the core. In the two extreme cases presented, a low temperature compared to terrestrial planets (lower than 1400 K) characterizes the core.

Different evolutions of the icy layers have been presented depending on the amount of ammonia. A thick internal liquid layer is predicted because the presence of ammonia decreases the melting temperature of the liquid layer. Compared to the pure water case, convective motions in the ice I layer are very weak because the viscosity is too large. The consequence is that for some critical thickness of the ice I layer, which depends on the initial amount of ammonia, a thermal equilibrium between the ice I layer and the core appears. Thickness of both the icy layers and the liquid layer no longer evolve rapidly with time, but have a very slow evolution in order to keep a thermal equilibrium with the core. Gravitational data from the Cassini orbiter will provide valuable information about the internal structure of Titan. More precise measurements than the Galileo spacecraft will be provided and should allow a good assessment of the internal structure of Titan. If a thick liquid layer is detected, its thickness will in turn provide constraints on its composition.

For understanding the influence of volatiles on the internal structure of Titan, more experimental data are required. Experimental works for nitrogen–water, methane–water and ammonia–methane–water systems at high pressures and low temperatures have to be conducted. Salty systems are not well known and could be good analogs of the liquid layers of icy satellites. Finally, even the ammonia–water system is not completely understood and may require further studies. A precise understanding of the different events occurring in the icy layers and the liquid layer of Titan will only be possible if all these experimental works are conducted.

Acknowledgements

This work has been partly funded by CNRS-CNES "Programme National de Planétologie". We thank the two reviewers who provided thorough and helpful comments.

References

Anderson, J.D., Lau, E.L., Sjogren, W.L., Schubert, G., Moore, W.B., 1996. Gravitational constraints on the internal structure of Ganymede. Nature 384, 541–544.

Bercovici, D., Schubert, G., Reynolds, R.T., 1986. Phase transitions and convection in icy satellites. Geophys. Res. Lett. 13 (5), 448–451.

Boehler, R., 1992. Melting of the Fe–FeO and the Fe–FeS systems at high pressure: constraints on core temperatures. Earth Planet. Sci. Lett. 111, 217–227.

Booker, J.R., 1976. Thermal convection with strongly temperature-dependent viscosity. J. Fluid Mech. 76, 741–754.

Boone, S., Nicol, M.F., 1991. Ammonia–water mixtures at high pressures: melting curves of ammonia dihydrate and ammonia monohydrate and a revised high pressure phase diagram for the water rich region. Proc. Lunar Planet. Sci. 21, 603–610.

Carslaw, H.S., Jaeger, J.C., 1959. Conduction of Heat in Solids. Oxford University Press, pp. 230–255.

Cassen, P.M., Peale, S.J., Reynolds, R.T., 1982. Structure and thermal evolution of the Galilean satellites. In: Morrison, D. (Ed.), Satellites of Jupiter. University of Arizona Press, Tucson, pp. 93–128.

Chizhov, V.E., 1993. Thermodynamic properties and thermal equation of state of high-pressure ice phases. Prikladnay Mekhanika i tekhnicheskaya Fizika 2, 113–123.

Choblet, G., Grasset, O., Parmentier, E.M., Sotin, C., 1999. Mars thermal evolution revisited. Lunar Planet. Sci. Conf. XXX, 1556–1557.

Christensen, U.R., 1984. Heat transport by variable viscosity convection and implications for the Earth's thermal evolution. Phys. Earth Planet. Int. 35, 264–282.

Christensen, U.R., 1985. Thermal evolution models for the Earth. J. Geophys. Res. 90, 2995–3007.

Cole, G.H.A., 1984. Comments on the differentiation of icy satellites. Geophys. J. Roy. Astr. Soc. 77, 549–557.

Consolmagno, G.J., Lewis, J.S., 1978. The evolution of icy satellites interiors and surfaces. Icarus 34, 280–293.

Coradini, A., Costanzo, F., Forni, O., Magni, G., 1995. Origin and thermal evolution of icy satellites. Surv. Geophys. 16, 533–591.

Davaille, A., Jaupart, C., 1993. Transient high Rayleigh number thermal convection with large viscosity variations. J. Fluid. Mech. 253, 141–166.

Deschamps, F., Sotin, C., 2000. Inversion of 2D numerical experiments for a strongly temperature-dependent viscosity fluid. Phys. Earth Planet. Int., in press.

Duhram, W.B., Kirby, S.H., Stern, L.A., 1993. Flow of ices in the ammonia–water system. J. Geophys. Res. 98 (17), 667–682.

Echelmeyer, K., Kamb, B., 1986. Rheology of ice II and ice III from high pressure extrusion. Geophys. Res. Lett. 13 (7), 693–696.

Forni, O., Federico, C., Coradini, A., Magni, G., 1998. Origin and evolution of comets, icy planets and satellites. In: Schmitt, B., De Bergh, C., Festou, M. (Eds.), Solar System Ices. Kluwer, pp. 367–394.

Friedson, A.J., Stevenson, D.J., 1983. Viscosity of rock–ice mixtures and applications to the evolution of icy satellites. Icarus 56, 1–14.

Gerrard, J.A.F., Perutz, M.F., Roch, A., 1952. Measurement of the velocity distribution along a vertical line through a glacier. Proc. Roy. Soc. A 207, 554–572.

Goldsby, D.L., Kolhstedt, D.L., 1997. Grain boundary sliding in fine-grained Ice-I. Scripta Materiala 37, 1399–1405.

Goodman, D.J., Frost, H.J., Ashby, M.F., 1981. The plasticity of polycristalline ice. Phil. Mag. A 43, 665–695.

Grasset, O., Sotin, C., 1996. The cooling rate of a liquid shell in Titan's interior. Icarus 123, 101–112.

Grasset, O., Parmentier, E.M., 1998. Thermal convection in a volumetrically heated, infinite Prandtl number fluid with strongly temperature dependent viscosity: implications for planetary thermal evolution. J. Geophys. Res. 103 (B8), 18171–18181.

Grasset, O., Beauchesne, S., Sotin, C., 1995. Investigation of the NH_3–H_2O phase diagram in the range 100 MPa–1.5 GPa using in-situ Raman spectroscopy: application to Titan's dynamics. Compt. Rend. Acad. Sci. 320 (IIa), 249–256.

Hanel, R., Conrath, B., Flasar, F.M., Kunde, V., Maguire, W., Pearl, J., Pirraglia, J., Samuelson, R., Herath, L., Allison, M., Cruikshank, D., Gautier, D., Guierasch, P., Horn, L., Koppany, R., Ponnamperuna, C., 1981. Infrared observations of the saturnian system from Voyager 1. Science 212, 192–200.

Hill, M.N., 1962. The Sea. Interscience, New York, p. 27.

Hobbs, P.V., 1974. Ice Physics. Clarendon Press, Oxford.

Hogenboom, D.L., Kargel, J.S., Consolmagno, G., Holden, T.C., Lee, L., Buyyounouski, M., 1997. The ammonia–water system and the chemical differentiation of icy satellites. Icarus 128, 171–180.

Javoy, M., 1995. The integral enstatite chondrite model of the earth. Geophys. Res. Lett. 22 (16), 2219–2222.

Johnson, M.L., Nicol, M., 1987. The ammonia–water phase diagram and its implications for icy satellites. J. Geophys. Res. 92, 6339–6349.

Kargel, J.S., 1992. Ammonia–water volcanism on icy satellites: phase relations at 1 atmosphere. Icarus 100, 556–574.

Kargel, J.S., 1998. Physical chemistry of ices in the outer solar system. In: Schmitt, B., De Bergh, C., Festou, M. (Eds.), Solar System Ices. Kluwer, pp. 3–32.

Kargel, J.S., Croft, S.K., Lunine, J.I., Lewis, J.S., 1991. Rheological properties of ammonia–water liquids and crystal–liquid slurries: planetological applications. Icarus 89, 93–112.

Khurana, K.K., Kivelson, M.G., Stevenson, D.J., Schubert, G., Russell, C.T., Walker, R.J., Polanskey, C., 1998. Induced magnetic fields as evidence for subsurface oceans in Europa and Callisto. Nature 395, 777–780.

Kirby, S.H., Durham, W.B., Heard, H.C., 1985. Rheologies of H_2O ices Ih, II and III at high pressures: a progress report. In: Klinger, J., Benest, B., Dollfus, A., Smoluchowski, R. (Eds.), Proceedings of NATO Workshop Ices in the Solar System. D. Reidel, Dordrecht, pp. 89–107.

Kirk, R.L., Stevenson, D.J., 1987. Thermal evolution of a differentiated Ganymede and implications for surface features. Icarus 69, 91–134.

Kivelson, M.G., Khurana, K.K., Russell, C.T., Walker, R.J., Warnecke, J., Coroniti, F.V., Polanskey, C., Southwood, D.J., Schubert, G., 1996. Discovery of Ganymede's magnetic field by the Galileo spacecraft. Nature 384, 537–541.

Kuramoto, K., Matsui, T., 1994. Formation of a hot proto-atmosphere on the accreting giant icy satellite: implications for the origin and evolution of Titan, Ganymede, and Callisto. J. Geophys. Res. 99 (E10), 21,183–21,200.

Lewis, J.S., 1971. Satellites of the outer planets: their physical and chemical nature. Icarus 15, 174–185.

Lunine, J.I., 1993. Does Titan have an ocean? A review of current understanding of Titan's surface. Rev. Geophys. 31 (2), 133–149.

Lunine, J.I., 1994. Does Titan have oceans? American Scientist 82, 134–143.

Lunine, J.I., Stevenson, D.J., 1987. Clathrates and ammonia hydrates at high pressure: application to the origin of methane in Titan. Icarus 70, 61–77.

Lupo, M.J., 1982. Mass–radius relationships in icy satellites after Voyager. Icarus 40, 157–170.

McCord, T.B., Hansen, G.B., Fanale, F.P., Carlson, R.W., Matson, D.L., Johnson, T.V., Smythe, W.D., Crowley, J.K., Martin, P.D., Ocampo, A., Hibbitts, C.A., Granahan, J.C., 1998. Salts on Europa's surface detected by Galileo's near infrared mapping spectrometer. Science 280, 1242–1245.

Moresi, L.N., Solomatov, V.S., 1995. Numerical investigation of 2D convection with extremely large viscosity variations. Phys. Fluids 7 (9), 2154–2162.

Morris, S.D., Canright, D., 1984. A boundary layer analysis of Benard convection in a fluid of strongly temperature-dependent viscosity. Phys. Earth Planet. Int. 36, 355–373.

Morrison, D., Owen, T., 1988. The Planetary System. Addison Wesley.

Mueller, S., McKinnon, W.B., 1988. Three layer Ganymedes and Callistos. Icarus 76 (3), 437–464.

Nataf, H.-C., 1991. Mantle convection, plates, and hotspots. Tectonophysics 187, 361–371.

Nataf, H.-C., Richter, F.M., 1982. Convection experiments with highly temperature-dependent viscosity and the thermal evolution of the planets. Phys. Earth Planet. Int. 32, 320–329.

Pappalardo, R.T., Head, J.W., Greeley, R., Sullivan, R.J., Pilcher, C., Schubert, G., Moore, W.B., Carr, M.H., Moore, J.M., Belton, M.J.S., Goldsby, D.L., 1998. Geological evidence for solid-state convection in Europa's ice shell. Nature 391, 365–368.

Poirier, J.P., 1982. Rheology of ices: a key to the tectonics of the ice moons of Jupiter and Saturn. Nature 299, 683–688.

Poirier, J.P., Shankland, T.J., 1993. Dislocation melting of iron and the temperature of the inner core boundary revisited. Geophys. J. Int. 115, 147–151.

Poirier, J.P., Sotin, C., Peyronneau, J., 1981. Viscosity of high pressure ice VI and evolution and dynamics of Ganymede. Nature 292, 225–227.

Rappaport, N., Bertotti, B., Giamperi, G., Anderson, J.D., 1997. Doppler measurements of the quadrupole moments of Titan. Icarus 126 (2), 313–323.

Reynolds, R.T., Cassen, P.M., 1979. On the internal structure of the major satellites of the outer planets. Geophys. Res. Lett. 6 (2), 121–124.

Richter, F.M., Nataf, H.C., Daly, S.F., 1983. Heat transfer and horizontally averaged temperature of convection with large viscosity variations. J. Fluid Mech. 129, 173–192.

Rollet, A.P., Vuillard, G., 1956. Sur un nouvel hydrate de l'ammoniac. C.R. Acad. Sci. Paris 243, 383–386.

Sagan, C., Thompson, W.R., 1984. Production and condensation of organic gases in the atmosphere of Titan. Icarus 59, 133–161.

Samuelson, R.E., Nath, R.N., Borysow, A., 1997. Gaseous abundances and methane supersaturation in Titan's troposphere. Planet. Space Sci. 45, 959–980.

Schubert, G., Cassen, P., Young, R.E., 1979. Subsolidus convecting cooling histories of terrestrial planets. Icarus 38, 192–211.

Schubert, G., Stevenson, D.J., Ellsworth, K., 1981. Internal structures of the Galilean satellites. Icarus 47, 46–59.

Sohl, F., Sears, W.D., Lorenz, R.D., 1995. Tidal dissipation on Titan. Icarus 115, 278–294.

Solomatov, V.S., 1995. Scaling of temperature and stress dependent viscosity convection. Phys. Fluids 7 (2), 266–274.

Sotin, C., Labrosse, S., 1999. Three dimensional thermal convection in an iso-viscous, infinite Prandtl number fluid heated from within and from below: applications to the transfer of heat through planetary mantles. Phys. Earth Planet. Int. 112 (34), 171–190.

Sotin, C., Parmentier, E.M., 1989. On the stability of a fluid layer containing a univariant phase transition: application to planetary interiors. Phys. Earth Planet. Int. 55, 10–25.

Sotin, C., Poirier, J.P., 1987. Viscosity of ice V. Journal de Physique 48, C1.233–C1.238.

Sotin, C., Gillet, P., Poirier, J.P., 1985. Creep of high-pressure ice VI. In: Klinger, J., et al. (Eds.), Ices in the Solar System. Reidel, pp. 109–118.

Sotin, C., Grasset, O., Beauchesne, S., 1998. Thermodynamic properties of high pressure ices: implications for the dynamics and internal structure of large icy satellites. In: Schmitt, B., De Bergh, C., Festou, M. (Eds.), Solar System Ices. Kluwer, pp. 79–96.

Stevenson, D.J., 1996. When Galileo met Ganymede. Nature 384, 511–512.

Thompson, W.R., Henry, T.J., Schwartz, J.M., Khare, B.N., Sagan, C., 1991. Plasma discharges in N_2+CH_4 at low pressures: experimental results and applications to Titan. Icarus 90, 57–73.

Tozer, D.C., 1972. The present thermal state of the terrestrial planets. Phys. Earth Planet. Int. 6, 182–197.

Turcotte, D., Schubert, G., 1982. Geodynamics: Applications of Continuum Physics to Geological Problems. Wiley, New York.

Tyler, G.L., Eshleman, V.R., Anderson, J.D., Levy, G.S., Lindal, G.F., Wood, G.E., Croft, T.A., 1981. Radio science investigations of the Saturn system with Voyager 1: preliminary results. Science 212, 201–206.

Urakawa, S., Kato, M., Kumazawa, M., 1987. Experimental study on the phase relations in the system Fe–Ni–O–S up to 15 GPa. In: Manghani, M.H., Syono, Y. (Eds.), High Pressure Research in Mineral Physics, pp. 95–111.

Wasson, J.T., Kalleymen, G.W., 1988. Composition of chondrites. Phil. Trans. Roy. Soc. London A325, 535–544.

Weber, P., Machetel, P., 1992. Convection within the inner-core and thermal implications. Geophys. Res. Lett. 19 (21), 2107–2110.

Weertman, J., 1973. Creep of ice. In: Whalley, E., Jones, S.J., Gold, L.W. (Eds.), Physics and Chemistry of Ice. Royal Society of Canada, Ottawa.

Weertman, J., 1983. Creep deformation of ice. Ann. Rev. Earth Planet. Sci. 11, 215–240.

Yarger, J., Lunine, J.I., Burke, M., 1993. Calorimetric studies of the ammonia–water system with application to the outer solar system. J. Geophys. Res. 98, 13,109–13,117.